Seismic Performance of Precast Reinforced Concrete Core Wall with Horizontal Tied Rebars at Mid Height Level of First Story

Tadaharu Nakachi*

Abstract: Precast core walls are considered effective for construction because they can be built more quickly than cast-in-place core walls. Previously, we conducted a lateral loading test on a full precast wall column simulating the area near the corner of an L-shaped core wall in order to examine the seismic performance. The wall column was divided into precast columns, and horizontal tied rebars were concentrated at the second and third floor levels to connect the precast columns. In this study, a lateral loading test was conducted on a wall column to which horizontal tied rebars were added at the mid height level of the first story. Based on the results of the test, the seismic performance of the wall column was clarified.

Keywords: Reinforced concrete, core wall, precast, horizontal tied rebar, cotter

1. INTRODUCTION

Multistory core walls installed in high-rise reinforced concrete buildings effectively reduce seismic vibration. On the other hand, precast core walls are considered effective for construction because they can be built more quickly than cast-in-place core walls. Previously, we conducted a lateral loading test on a full precast wall column simulating the area near the corner of an L-shaped core wall.[1)] The specimen consisted of four square-section precast columns. The vertical joints between the precast columns were grouted with high-strength mortar. Each precast column had cotters at the vertical joint. Horizontal tied rebars were concentrated at the second and third floor levels to connect the precast columns. In this study, a lateral loading test was conducted on a wall column to which horizontal tied rebars were added at the mid height level of the first story.

2. SUMMARY OF TEST

2.1 Test Specimen

The configuration and arrangement of reinforcement in the specimen are shown in Fig. 1. The physical properties of the concrete and reinforcement are listed in Table 1 and Table 2, respectively. A one-eighth-scale precast wall column Specimen PC2 simulating the area near the corner of an L-shaped core wall was tested. The specimen represented the lower three stories of a high-rise building of approximately 25 stories. The specimen had a rectangular cross section measuring 90 × 405 mm, was the flexural type and had a shear span ratio of 2.4. The specimen consisted of four

* Department of Architecture and Environmental Engineering

square-section precast columns arranged in a line. The width of the opening between columns was 7 mm, and the openings were grouted. Each precast column had cotters without cotter bars at the vertical joint, and the depth of the cotter was 6 mm. The specified design strength of the concrete was 60 N/mm^2, and that of the grout was 80 N/mm^2. D10 deformation bars with yield strength of 397 N/mm^2 were used for the main bars of the precast columns and the horizontal tied rebars. High-strength U5.1 bars with a yield strength of 1368 N/mm^2 were used for the hoops of the precast columns. The pitch of the hoop was 55 mm. The specimen cover concrete was 6 mm thick.

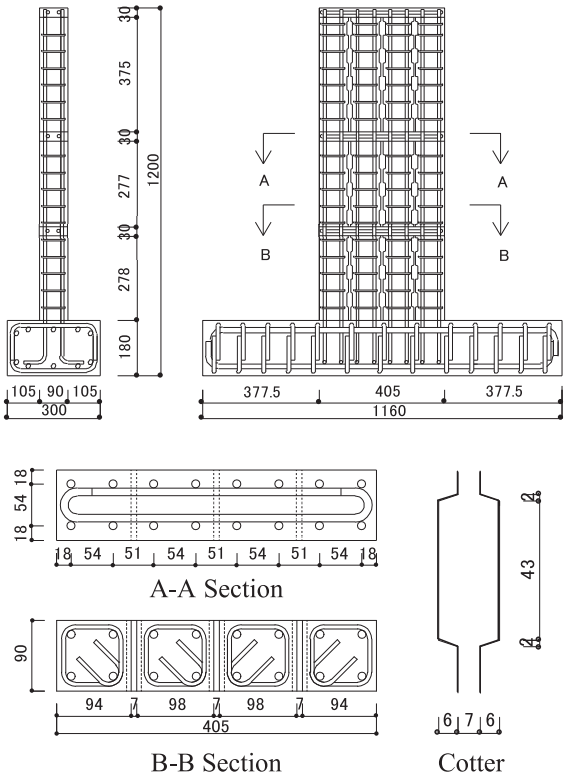

Fig. 1 Test Specimen

The concrete for the second and third floors was cast after the vertical joints of the precast columns were grouted. The horizontal tied rebars were concentrated at the floor level to connect the precast columns. Furthermore, the columns at the first story were divided into two parts at the mid height level of the first story and the concrete for the area between the two parts was cast. The horizontal tied rebars were concentrated at the area between the two parts the same as at the second and third floor levels. Therefore, in this study, integration of precast columns was enhanced in Specimen PC2 by the horizontal tied rebars added at the mid height level of the first story, compared with Specimen PC1 which was tested last year.

Table 1 Physical Properties of Concrete

	Compressive Strength (N/mm^2)	Young's Modulus (×10^{4}N/mm^2)	Sprit Strength (N/mm^2)
Precast	60.6	2.63	2.75
Latter	58.7	2.65	2.13
Grout	91.7	3.24	4.85

Table 2 Physical Properties of Steel

Bar Size	Yield Strength (N/mm^2)	Maximum Strength (N/mm^2)	Young's Modulus (×10^{5}N/mm^2)	Elogation (%)
D10	397	577	1.85	18.5
U5.1	1368	1491	2.11	9.3

2.2 Test Procedure

The loading test was a cantilever type, as shown in Fig. 2. In the cyclic lateral loading test, the specimen was subjected to lateral forces by a horizontal hydraulic jack connected to the reaction frame. Positive loading was conducted by pulling the PC steel bars with the jack. The PC steel bars were attached to the pin support on the right side of the specimen (Fig. 2). Therefore, the specimen

was pushed from the right side. Loading was conducted without tying the precast columns with the PC steel bars. Negative loading was conducted by pushing the specimen with the jack from the left side. A constant axial loading force was applied by a vertical hydraulic jack over the specimen to represent the axial stress in the stage of coupling beam yielding at the center core. The axial stress was 20% of the concrete compressive cylinder strength. Loading was controlled by the horizontal drift angle at a height corresponding to the second floor level (h: 615 mm). The loading was cyclic lateral loading at R (drift angle) = 1/1000 (rad.) (1 cycle), 2/1000, 5/1000, 7.5/1000, 10/1000, 15/1000, 20/1000 (2 cycle respectively), 30/1000 (1 cycle). The relative displacement was measured by displacement transducers, such as the expansion and contraction of each segment and the relative sliding and opening displacement in the vertical joints. Strain gages were attached to the hoop, the horizontal tied rebars and the main bars. The attachment position of strain gages at the hoop was the midpoint of the side.

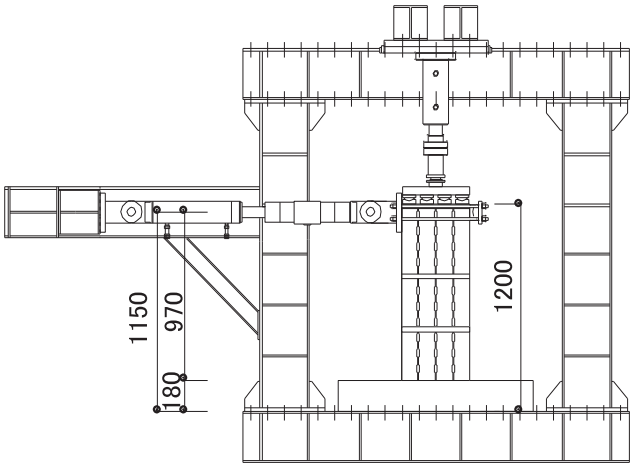

Fig. 2 Loading System

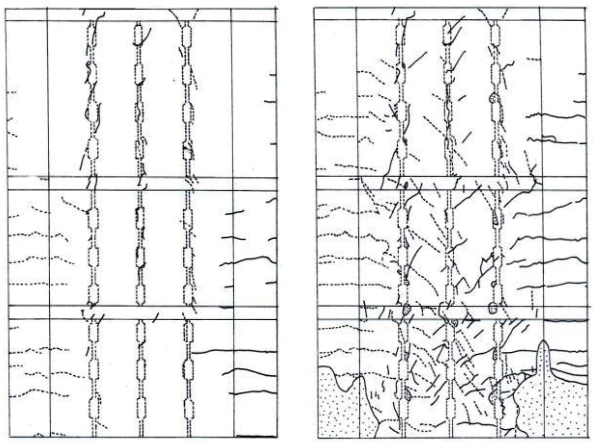

R = 5/1000rad. Final Stage

Fig. 3 Crack Patterns

3. TEST RESULTS

3.1 Fracture Process

The crack patterns of the specimen at 5/1000 and the final stage are shown in Fig. 3. Under both positive and negative loadings, flexural cracks occurred by 2/1000 at the bottom of the specimen. The flexural cracks then expanded upward and to the middle of the specimen. Shear cracks occurred at the cotter by 5/1000 and then extended. Under both positive and negative loadings, flexural shear cracks occurred by 5/1000. The corner area at the bottom appeared to crack vertically and crumbled slightly by 5/1000. After 7.5/1000, expansion of shear cracks at the cotter was not large, and flexural cracks, flexural shear cracks and crumbling of concrete at the bottom expanded. During the cycle of 30/1000, the strength decreased slightly, when a slight opening between the grout and concrete at the cotter was observed. With regard to the yield of reinforcement, the main bar at the compressive

end yielded (yield strain 2146 × 10^{-6}) by 7.5/1000 under positive loading, and the main bar at the tensile end yielded by 15/1000. The specimen maintained the axial load by the final cycle at 30/1000.

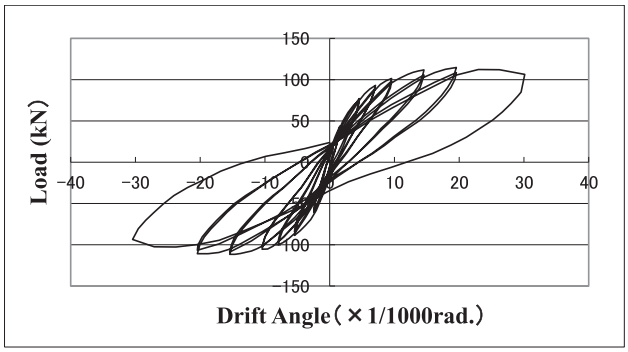

Fig. 4 Load - Deflection Curve

3.2 Load–Deflection Curves

Figure 4 shows the load–deflection curves. The maximum strength of positive loading was 114.8 kN at 20/1000, and that of negative loading was 111.5 kN at 15/1000. The strength decreased slightly during the last cycle of 30/1000 under both positive and negative loadings.

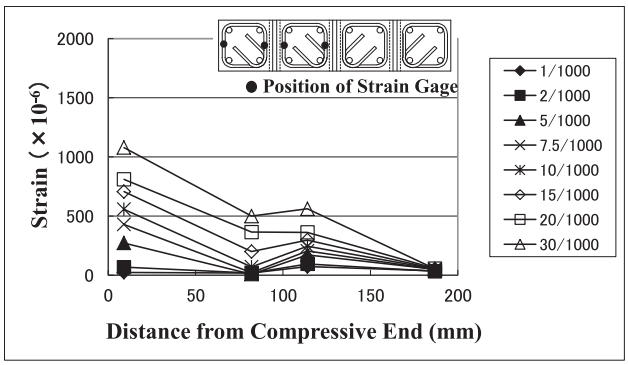

Fig. 5 Horizontal Strain Distribution of Hoop (Height of 42.5 mm)

3.3 Strain Distribution of Hoop (Measuring Point in Thickness Direction)

3.3.1 Horizontal strain distribution

Figures 5 and 6 show the horizontal strain distribution of the hoop at heights of 42.5 and 152.5 mm, respectively. The strain was measured by strain gages attached to both sides of the hoop at the neutral axis, and the strain values are the average of both sides. The attachment position of strain gages at the hoop was the midpoint in the thickness direction of the specimen. The thickness direction is perpendicular to the loading direction, so the value of the measuring point in the thickness direction is considered to indicate the confinement effect of concrete on the vertical compressive stress rather than the shear reinforcing effect on the lateral force. The distribution was longitudinal in the cross section of the specimen, and at the peak of positive loading for each drift angle. The figures show the relationship between the strain of the hoop and the distance from the compressive end.

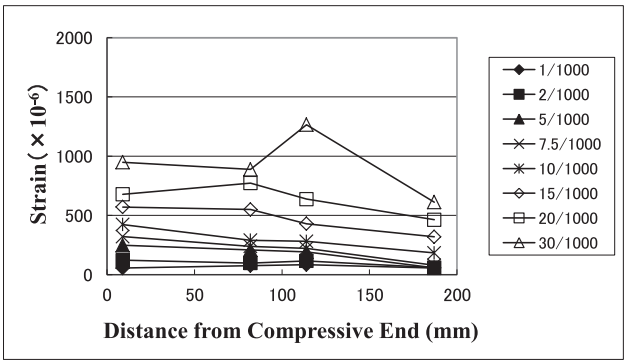

Fig. 6 Horizontal Strain Distribution of Hoop (Height of 152.5 mm)

Strain increased with the increase in drift angle at all measuring points at both heights. At a height of 42.5 mm, the values at the point 9 mm from the compressive end were the largest, and the nearer the point was to the compressive end, the larger the value. The increase in strain at the points 187

mm from the compressive end with the increase in drift angle was small. On the other hand, strain at the points 9 mm to 114 mm from the compressive end increased with the increase in drift angle. Especially after 15/1000, not only strain of the column at the compressive end but also that of the column next to the column at the compressive end increased. Strain of both these columns had a tendency of decreasing gradually from the compressive end to the middle of the specimen.

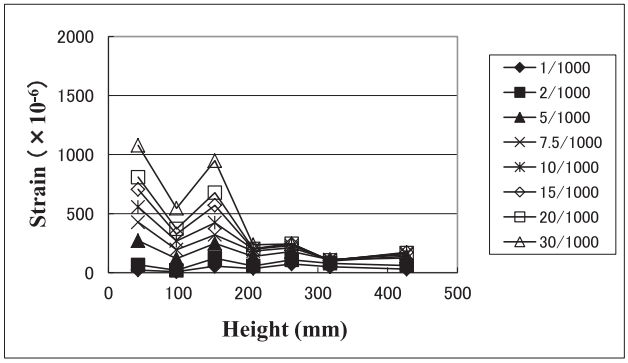

Fig. 7 Vertical Strain Distribution of Hoop

At a height of 152.5 mm also, strain decreased gradually from the compressive end to the middle of the specimen. Therefore, it is considered that the compressive stress condition of the column at the compressive end and the next column is unified. The value at the point 187 mm from the compressive end was larger than that at a height of 42.5 mm. This is considered to show the large compressive stress at the wider area up to the middle of the specimen. However, at the final stage of 30/1000, strain of the column at the compressive end and the next one was larger nearer the compressive end. This shows that the compressive stress of both these columns tended to be somewhat independent.

3.3.2 Vertical strain distribution

Figure 7 shows the vertical strain distribution of the hoop at the measuring point 9 mm from the compressive end. The figure shows the relationship between the strain of the hoop and the height from the bottom at the peak of positive loading for each drift angle. Strain increased near the bottom as a whole. Up to 5/1000, the strain increased at an approximately constant rate toward the bottom. On the other hand, after 7.5/1000, the increment of strain near the bottom was remarkable at heights below 200 mm. During the fracture process mentioned above, the main bar at the compressive end yielded by 7.5/1000, and the corner area at the bottom appeared to crack vertically and crumbled slightly by 5/1000. From the fracture process and vertical strain distribution of the hoop, it is considered that the concrete at the compressive end was elastic at all heights up to 5/1000 and a range of approximately 200 mm at the bottom became plastic after 7.5/1000.

3.4 Strain Distribution of Horizontal Tied Rebars

Figures 8, 9 and 10 show the strain distribution of the horizontal tied rebars at the mid height level of the first story, heights corresponding to the second and third floor levels, respectively. Strain increased with the increase in drift angle at all measuring points at any level. The strain at the

compressive end side was larger than that at the tensile end side as a whole. At the mid height level of the first story, the strain increased remarkably at a drift angle of 2/1000 to 5/1000. The strain at the point 93 mm from the compressive end, that is, the strain at the point on the boundary between the column at the compressive end and the next column, exceeded the yield strain and increased dramatically at 30/1000. On the load–deflection curves, the strength decreased slightly during the last cycle of 30/1000. It is considered that the reason for this decrease was a decline of unification and the independent movement of both these columns by yielding of the horizontal tied rebars at this boundary point. At the second floor level, the strain distribution is almost the same and the value of strain is slightly smaller than that of the mid height level of the first story. There was no yielding until the last cycle of 30/1000. At the third floor level, the value of strain was smaller than that of the other levels. However, the strain at the point 149.5 mm from the compressive end exceeded the yield strain.

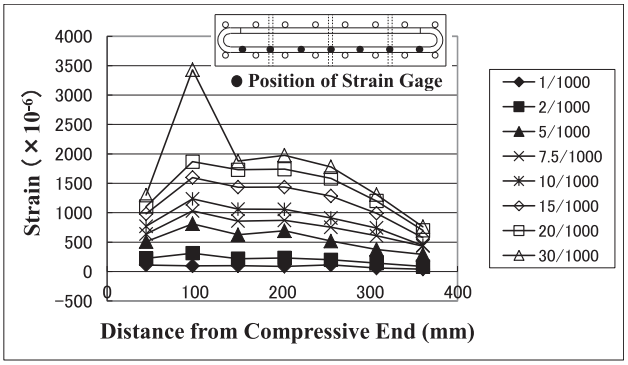

Fig. 8 Strain Distribution of Horizontal Tied Rebars (Mid Height Level of First Story)

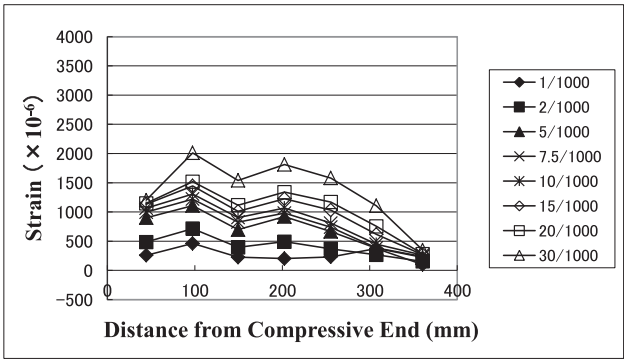

Fig. 9 Strain Distribution of Horizontal Tied Rebars (Second Floor Level)

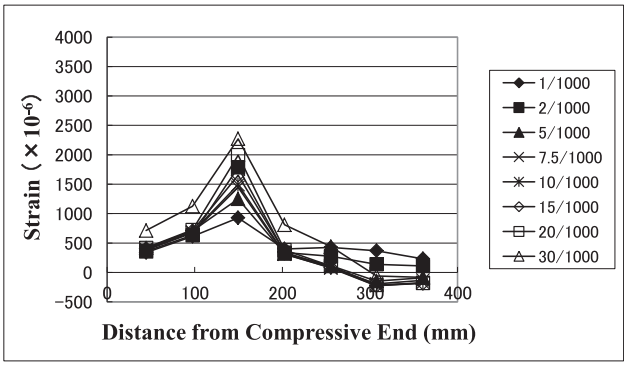

Fig. 10 Strain Distribution of Horizontal Tied Rebars (Third Floor Level)

3.5 Horizontal Distribution of Vertical Strain at the Bottom

Figure 11 shows the horizontal distribution of the vertical strain measured by displacement transducers. The measuring length was 65 mm. The figure shows the relationship between the vertical strain and the distance from the compressive end at the peak of positive loading for each drift angle. The strain changed from compressive to tensile between the compressive end and tensile end as a whole up to 10/1000. On

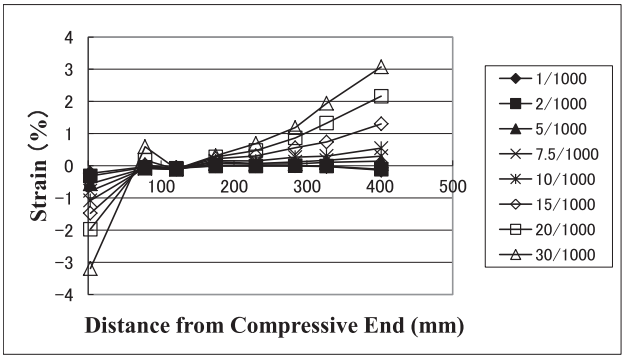

Fig. 11 Horizontal Distribution of Vertical Strain at Bottom

the other hand, the tensile strain at the point 78 mm from the compressive end increased remarkably after 20/1000. That is, independent movement was observed at the bottom of the precast column at the compressive end.

3.6 Sliding and Opening in the Vertical Joint

3.6.1 Horizontal distribution of opening

Figures 12, 13 and 14 show the horizontal distribution of the opening in the vertical joint between the precast columns under positive loading. In the figure, the first, second and third array show the horizontal distribution at the lower part of the first story (height 170 mm), the upper part of the first story (height 415 mm) and the middle part of the second story (height 805 mm), respectively. The horizontal relative displacement between the precast columns was measured by the displacement transducer as the opening. The opening increased with the increase in the drift angle at any array.

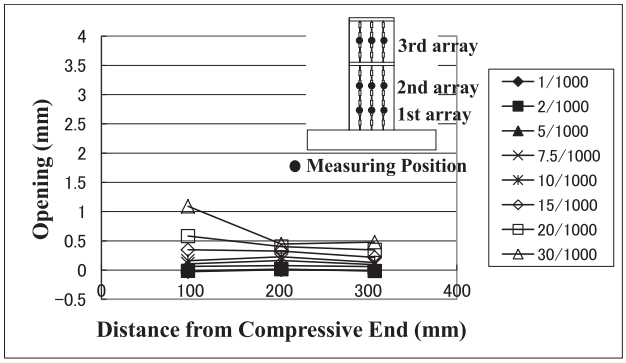

Fig. 12 Horizontal Distribution of Opening (First Array)

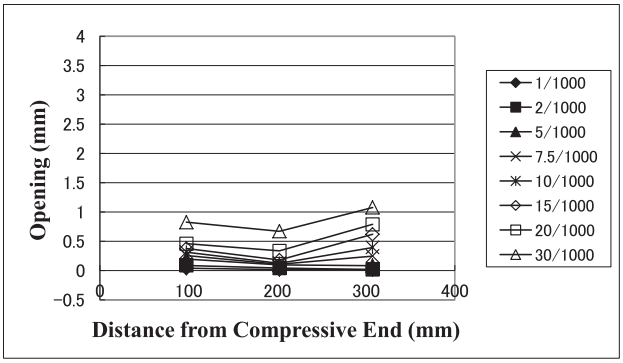

Fig. 13 Horizontal Distribution of Opening (Second Array)

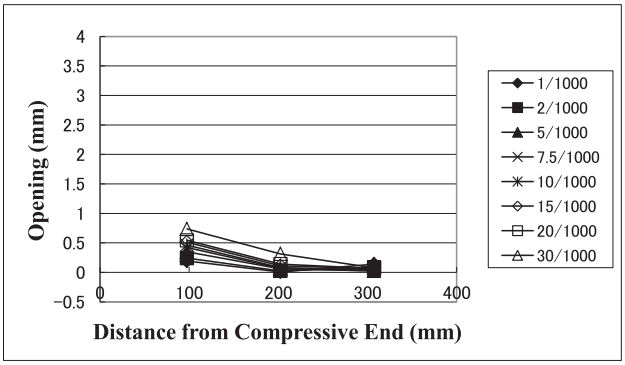

Fig. 14 Horizontal Distribution of Opening (Third Array)

At the first array, the increase in the opening was small up to 10/1000, but the opening increased greatly after 15/1000. Comparing in the horizontal direction, the opening was larger on the compressive side especially after 15/1000. The opening increased remarkably at a drift angle of 20/1000 to 30/1000 on the compressive side. The largest opening was 1.1 mm in width on the compressive side at 30/1000. At the second array, the increase in the opening was small up to 5/1000, but the opening increased greatly especially on the tensile side after 7.5/1000. Comparing in the horizontal direction, the opening of both sides was larger than that of the midpoint. This tendency was remarkable after 7.5/1000. The distribution was approximately symmetric after 7.5/1000. The opening increased remarkably at a drift angle of 20/1000 to 30/1000 as a whole. The largest opening was 1.1 mm in width on the tensile side at 30/1000. At the third array, the opening increased up to 1/1000 and at 2/1000 to 5/1000 on the compressive side, and hardly increased on the tensile side.

Comparing in the horizontal direction, the opening was larger on the compressive side. The opening increased remarkably on the compressive side and at the midpoint at a drift angle of 20/1000 to 30/1000. The largest opening was 0.7 mm in width on the compressive side at 30/1000.

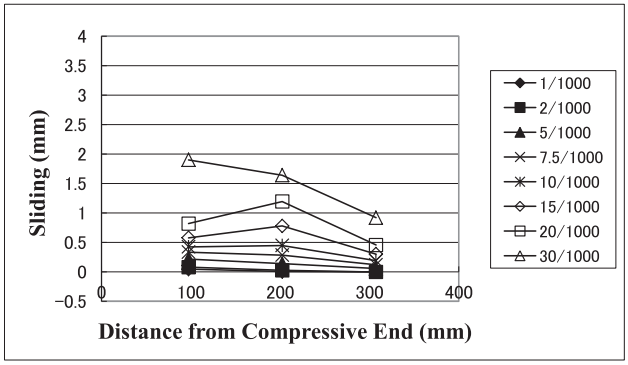

Fig. 15 Horizontal Distribution of Sliding (First Array)

A comparison of the openings by the average value of each array revealed the following. The opening of the second array was largest and that of the first array was the second largest. With regard to the horizontal distribution of the opening, the opening on the compressive side was largest and decreased toward the tensile side at the first and third arrays. On the other hand, the openings on both sides were larger than that at the midpoint at the second array. The opening increased remarkably at any array at a drift angle of 20/1000 to 30/1000.

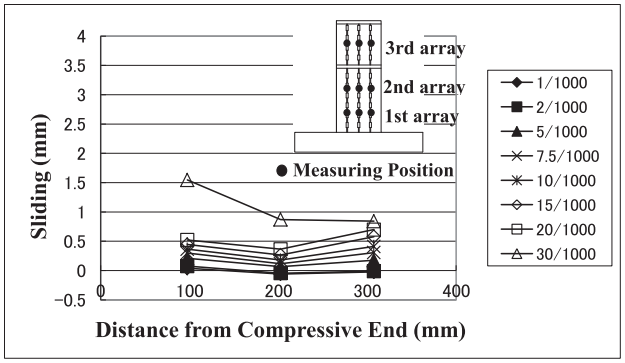

Fig. 16 Horizontal Distribution of Sliding (Second Array)

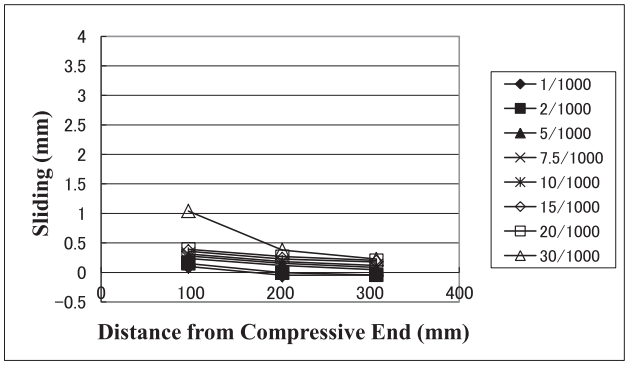

Fig. 17 Horizontal Distribution of Sliding (Third Array)

3.6.2 Horizontal distribution of sliding

Figures 15, 16 and 17 show the horizontal distribution of sliding at the vertical joint between the precast columns under positive loading. The measuring point of sliding corresponds to that of the opening mentioned above. The vertical relative displacement between the precast columns was measured by the displacement transducer as the sliding. Positive sliding was defined as the case of sliding up on the compressive side in the vertical joint under positive loading. The sliding increased with the increase in the drift angle at any array.

At the first array, the increase in the sliding was small up to 2/1000, but the sliding increased largely after 5/1000. Comparing in the horizontal direction, the sliding was larger on the compressive side up to 7.5/1000, and at the midpoint after 10/1000. The sliding increased remarkably on the compressive side at a drift angle of 20/1000 to 30/1000 and was largest on the

compressive side again at 30/1000. The largest sliding was 1.9 mm on the compressive side at 30/1000. At the second array, the increase in the sliding was small up to 2/1000, but the sliding increased largely after 5/1000 the same as the sliding at the first array. Comparing in the horizontal direction, the sliding of both sides was larger than that of the midpoint, unlike at the first array. This tendency was shown from the first stage of 1/1000 and the distribution was approximately symmetric. This tendency of symmetry corresponded to that of the opening measured at the same second array. However, the sliding increased remarkably on the compressive side and at the midpoint at a drift angle of 20/1000 to 30/1000 and was largest on the compressive side at 30/1000. The largest sliding was 1.5 mm on the compressive side at 30/1000. At the third array, the sliding increased gradually up to 20/1000. Comparing in the horizontal direction, the sliding was larger on the compressive side. The sliding increased remarkably on the compressive side at a drift angle of 20/1000 to 30/1000 and the largest sliding was 1.0 mm on the compressive side at 30/1000.

A comparison of the sliding by the average value of each array revealed the following. The sliding of the first array was largest and that of the second array was the second largest. This tendency was different from that of the opening. The opening was largest at the second array. Comparing in the horizontal direction up to 20/1000, the largest sliding was at the midpoint, both sides and the compressive side at first, second and third arrays, respectively, that is, the tendency differed among the arrays. On the other hand, the sliding increased largely to approximately double on the compressive side at a drift angle of 20/1000 to 30/1000. As a result, the sliding on the compressive side was largest and decreased toward the tensile side at any array at 30/1000.

4. CONCLUSIONS

A lateral loading test on full precast wall columns simulating the area near the corner of an L-shaped core wall was conducted in order to examine the seismic performance. Major findings are as follows:

(1) In the vertical strain distribution of the hoop, the increment of strain near the bottom was remarkable at a height below 200 mm after 7.5/1000. This area corresponded to the crumbling area in the fracture process. It is considered that a range of approximately 200 mm at the bottom became plastic after 7.5/1000.

(2) In the horizontal distribution of vertical strain at the bottom, the tensile strain at the point 78 mm from the compressive end increased remarkably after 20/1000. That is, independent movement was observed at the bottom of the precast column at the compressive end.

(3) The opening in the vertical joint was largest at the upper part of the first story. The largest value

of opening was 1.1 mm, and the distribution of the opening was symmetric on the compressive side and the tensile side. The sliding in the vertical joint was largest at the lower part of the first story. The largest value of sliding was 1.9 mm, and the distribution of the sliding was larger on the compressive side.

ACKNOWLEDGEMENT

This work was supported by JSPS KAKENHI (23560683).

REFERENCES

1) Nakachi, T., Tokunaga, R. (2012). Experimental Study on Structural Performance of Precast Reinforced Concrete Core Walls (Part 1, Part 2). *Summaries of Technical Papers of Annual Meeting of Architectural Institute of Japan*, 367-370.

（平成 25 年 3 月 31 日受理）